ASME 2003 Design Engineering Technical Conferences and
Computers and Information in Engineering Conference
Chicago, Illinois, USA, September 2-6, 2003

DETC2003/VIB-48353

A NEW TYPE COMPONENT MODE SYNTHESIS BEAM ELEMENT BASED ON THE ABSOLUTE NODAL COORDINATE FORMULATION

Riki Iwai
School of Integrated Design Engineering
Keio University
3-14-1 Hiyoshi, Kohoku-ku, Yokohama, 223-8522
JAPAN
Email: riki_iwai@hotmail.com

Nobuyuki Kobayashi
Department of Mechanical Engineering
Aoyama Gakuin University
5-10-1 Fuchinobe, Sagamihara, Kanagawa, 229-8558
JAPAN
Email: kobanobu@me.aoyama.ac.jp

ABSTRACT

This paper establishes a new type component mode synthesis method for a flexible beam element based on the absolute nodal coordinate formulation. The deformation of the beam element is defined as the sum of the global shape function and the analytical clamped-clamped beam modes. This formulation leads to a constant and symmetric mass matrix as the conventional absolute nodal coordinate formulation, and makes it possible to reduce the system coordinates of the beam structure which undergoes large rotations and large deformations. Numerical examples show that the excellent agreements are examined between the presented formulation and the conventional absolute nodal coordinate formulation. These results demonstrate that the presented formulation has high accuracy in the sense that the presented solutions are similar to the conventional ones with the less system coordinates and high efficiency in computation.

Keywords: flexible beam, large rotation, large deformation, component mode synthesis, absolute nodal coordinate formulation

INTRODUCTION

Recently, the absolute nodal coordinate formulation (A.N.C.F) [1] for formulating large rotation and large deformation problems of very flexible beam, plate and shell elements has been proposed. In this formulation, beams, plates and shells which have primarily been established as a non-isoparametric element are considered as an isoparametric element. Although the vector of nodal coordinates does not contain infinitesimal or finite rotation coordinates, global slope coordinates are used for an exact arbitrary rigid body description instead. Using the shape function of the conformal type that ensures the continuity of all the displacements, displacement gradients at nodal points and element interfaces in the analysis of two and three dimensional element, the center line and mid surface can be smooth. This kind of shape function satisfies both the compatibility conditions and the completeness conditions which imply one of the sufficient conditions for the convergence of finite element.

Two different methods can be used to derive the element elastic forces in A.N.C.F. In one method, the element coordinate system such as a pinned frame and a tangent frame that are used for the description of the element deformation is introduced. These element coordinate systems allow for the use of linear strain-displacement relationships [2–4].

Another method for deriving the elastic forces is to use a continuum mechanics approach (C.M.A) that does not require the use of a local element coordinate system. The beam element based on the assumption of Euler-Bernoulli beam model was established in the previous study of A.N.C.F [5, 6]. A more general longitudinal deformation model which does not employ the constant or the small strain assumptions was presented [6]. Omar [7] established a more general shear deformable beam element based on the nonlinear strain-displacement relationships, and Mikkola [8] developed it into three dimensional plate and

shell element. A new three dimensional beam element is now being developed [9]. Using C.M.A, much simpler elastic forces can be obtained than those of the former method using local element coordinate system. Moreover the solutions obtained by C.M.A converge well with small numbers of finite elements.

A.N.C.F tends to increase the number of degrees of freedom to be solved, as it is based on the finite element method. The reduced order formulation is desired to decrease the degrees of freedom. One of the present authors has developed a new type of component mode synthesis method (C.M.S) [10] where the displacement function of the linear beam finite element based on the classical Euler-Bernoulli beam theory is treated as a linear combination of the third order polynomials and the analytical clamped-clamped beam modes, and applied for the large rotation vector formulation [11]. Using this kind of C.M.S, mode truncations at nodal points can be prevented since the applied modes are chosen to the type of clamped beam that satisfies the boundary condition of zero displacement and zero slope at both ends.

In this study, we shed light on three kinds of the Euler-Bernoulli beam based element [2–5] in order to extend these models to the lower order and more accurate models with reduced number of system degrees of freedom in comparison with the conventional beam element based on A.N.C.F. Since the displacement function is modeled by using the constraint modes, the present shape function ensures the continuity of all the displacements and displacement gradients at nodal points. As a consequence, the presented beam element satisfies C^1 continuity condition and does not account for the shear deformation. In this paper, the accuracies of C.M.S based models are evaluated numerically by comparing with the large numbers of finite beam elements only based on the conventional A.N.C.F.

DERIVATION OF EQUATIONS OF MOTION BASED ON A.N.C.F USING C.M.S

Kinematic Equations

Figure 1 shows the planar beam element and the coordinate system used in this study. In A.N.C.F, the global position vector of an arbitrary point on the beam element based on the Euler-Bernoulli beam theory which does not account for the shear deformation is defined using the following equation:

$$\mathbf{r}^{ij} = \mathbf{S}^{ij}\mathbf{e}^{ij} \tag{1}$$

where $\mathbf{r}^{ij}$ is the global position vector of an arbitrary point on the beam element, $\mathbf{S}^{ij}$ is the element shape function matrix, $\mathbf{e}^{ij}$ is the vector of nodal coordinates, and superscript ij refers to element j on body i. We define the element shape function matrix $\mathbf{S}^{ij}$ and the vector of nodal coordinates $\mathbf{e}^{ij}$ which are based on C.M.S can

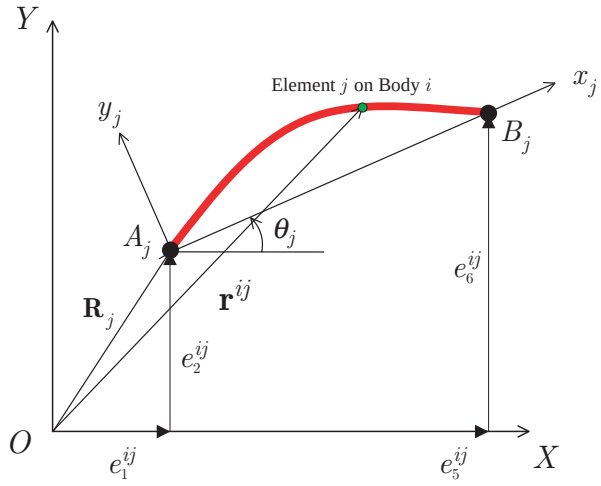

Figure 1. The planar beam element based on A.N.C.F & C.M.S

be written as follows:

$$\mathbf{S}^{ij} = \begin{bmatrix} 1-3\xi_j^2+2\xi_j^3 & 0 \\ l_j\left(\xi_j-2\xi_j^2+\xi_j^3\right) & 0 \\ 3\xi_j^2-2\xi_j^3 & 0 \\ l_j\left(\xi_j^3-\xi_j^2\right) & 0 \\ 0 & 1-3\xi_j^2+2\xi_j^3 \\ 0 & l_j\left(\xi_j-2\xi_j^2+\xi_j^3\right) \\ 0 & 3\xi_j^2-2\xi_j^3 \\ 0 & l_j\left(\xi_j^3-\xi_j^2\right) \\ \boldsymbol{\Phi}_X^{ij} & \mathbf{0} \\ \mathbf{0} & \boldsymbol{\Phi}_Y^{ij} \end{bmatrix}^T, \quad \xi_j = \frac{x_j}{l_j} \tag{2}$$

$$\mathbf{e}^{ij} = \left[\, e_1^{ij}\ e_3^{ij}\ e_5^{ij}\ e_7^{ij}\ e_2^{ij}\ e_4^{ij}\ e_6^{ij}\ e_8^{ij}\ \zeta_{X_1}^{ij}\cdots\zeta_{X_k}^{ij}\ \zeta_{Y_1}^{ij}\cdots\zeta_{Y_k}^{ij}\,\right]^T \quad (k=1,\ldots,n) \tag{3}$$

where l_j is the length of the element, x_j is the axial coordinate that defines the position of an arbitrary point on the element in the undeformed configuration, and $\boldsymbol{\Phi}_X^{ij}$, $\boldsymbol{\Phi}_Y^{ij}$ are the clamped-clamped beam mode vector defined as:

$$\boldsymbol{\Phi}_X^{ij} = \boldsymbol{\Phi}_Y^{ij} = \left[\, \phi_1(\xi_j)\cdots\phi_k(\xi_j)\,\right]^T \tag{4}$$

In Eq. 2, the two components of the displacement are interpolated using the same polynomials since these displacement components are defined in the global coordinate system. In Eq. 3, e_1^{ij} and e_2^{ij} are the translational coordinates at the node at point A_j as shown in Fig. 1, e_5^{ij} and e_6^{ij} are the translational coordinates at the node at point B_j, e_3^{ij} and e_4^{ij} are the global slope coordinates

at the node at point A_j, and e_7^{ij} and e_8^{ij} are the global slope coordinates at the node at point B_j, respectively. In addition to these components, $\zeta_{X_k}^{ij}$, $\zeta_{Y_k}^{ij}$ are the k th normal mode coordinates for the global X, Y directions of the element and $\phi_k(\xi_j)$ is the k th constraint mode.

It is note that when the A.N.C.F is used in this study, there is no reason for using different modes and different degrees of normal mode coordinates to describe different components of the displacements of the beam element since these components are defined in the global coordinate system. Therefore we use the same modes and the same numbers of modes to describe the global X, Y directions. By using the global slope coordinates as nodal coordinates in this formulation, it can be shown that the conventional modes of the beam can be used to define an isoparametric element in succession from the previous study based on A.N.C.F. The applied modes in this study must be chosen to avoid leading mode truncations at nodal points. This can be circumvented using the constraint modes like that of a clamped-clamped beam. As a consequence, the shape function developed in this study ensures continuity of all the displacements and displacement gradients at nodal points of the beam element. This continuity will be investigated numerically later in this paper.

For convenience of derivation of equations, we redefine the element shape function matrix $\mathbf{S}^{ij}$ in Eq. 2 as follows:

$$\mathbf{S}^{ij} = \left[\mathbf{S}_p^{ij} \ \boldsymbol{\Phi}_m^{ij} \right] = \begin{bmatrix} \mathbf{S}_{p1}^{ij} & \mathbf{0} & \boldsymbol{\Phi}_{m1}^{ij} & \mathbf{0} \\ \mathbf{0} & \mathbf{S}_{p2}^{ij} & \mathbf{0} & \boldsymbol{\Phi}_{m2}^{ij} \end{bmatrix} \equiv \begin{bmatrix} \mathbf{S}_1^{ij} \\ \mathbf{S}_2^{ij} \end{bmatrix} \tag{5}$$

Mass Matrix

Using Eq. 1, the kinetic energy of the beam element can be defined as:

$$T^{ij} = \frac{1}{2} \int_{V^{ij}} \rho^{ij} \dot{\mathbf{r}}^{ijT} \dot{\mathbf{r}}^{ij} dV^{ij} = \frac{1}{2} \dot{\mathbf{e}}^{ijT} \mathbf{M}^{ij} \dot{\mathbf{e}}^{ij} \tag{6}$$

where ρ^{ij} and V^{ij} are the mass density and volume of the finite element j of the deformable body i. $\mathbf{M}^{ij}$ is the constant symmetric mass matrix of the beam element using C.M.S proposed in this study, and can be defined as:

$$\begin{aligned} \mathbf{M}^{ij} &= \int_{V^{ij}} \rho^{ij} \mathbf{S}^{ijT} \mathbf{S}^{ij} dV^{ij} \\ &= m^{ij} \begin{bmatrix} \mathbf{M}_p^{ij} & \mathbf{M}_{pm}^{ij} \\ \mathbf{M}_{mp}^{ij} & \mathbf{M}_m^{ij} \end{bmatrix} \end{aligned} \tag{7}$$

The matrix $\mathbf{M}_p^{ij}$ in Eq. 7 can be written explicitly [1] as:

$$\mathbf{M}_p^{ij} = \begin{bmatrix} \mathbf{M}_{p1}^{ij} & \mathbf{0} \\ \mathbf{0} & \mathbf{M}_{p2}^{ij} \end{bmatrix} \tag{8}$$

$$\mathbf{M}_{p1}^{ij} = \mathbf{M}_{p2}^{ij} = \begin{bmatrix} \frac{13}{35} & \frac{11 l_j}{210} & \frac{9}{70} & -\frac{13 l_j}{420} \\ & \frac{l_j^2}{105} & \frac{13 l_j}{420} & -\frac{l_j^2}{140} \\ & & \frac{13}{35} & -\frac{11 l_j}{210} \\ Sym & & & \frac{l_j^2}{105} \end{bmatrix} \tag{9}$$

The matrices $\mathbf{M}_{pm}^{ij}$ and $\mathbf{M}_m^{ij}$ in Eq. 7 can be derived by integrating the clamped-clamped beam modes.

$$\begin{aligned} \mathbf{M}_{pm}^{ij} &= \mathbf{M}_{mp}^{ijT} = \begin{bmatrix} \mathbf{M}_{pm1}^{ij} & \mathbf{0} \\ \mathbf{0} & \mathbf{M}_{pm2}^{ij} \end{bmatrix} \\ &= \int_0^1 \mathbf{S}_p^{ijT} \boldsymbol{\Phi}_m^{ij} d\xi_j \end{aligned} \tag{10}$$

$$\begin{aligned} \mathbf{M}_m^{ij} &= \int_0^1 \boldsymbol{\Phi}_m^{ijT} \boldsymbol{\Phi}_m^{ij} d\xi_j \\ &= \int_0^1 \mathrm{diag}\left[\phi_1^2(\xi_j) \cdots \phi_k^2(\xi_j) \ \phi_1^2(\xi_j) \cdots \phi_k^2(\xi_j) \right] d\xi_j \end{aligned} \tag{11}$$

The applied modes $\phi_k(\xi_j)$ can be written explicitly as:

$$\begin{aligned} \phi_k(\xi_j) = C_k \big\{ &(\sinh \lambda_k - \sin \lambda_k)(\cosh \lambda_k \xi_j - \cos \lambda_k \xi_j) \\ &-(\sinh \lambda_k \xi_j - \sin \lambda_k \xi_j)(\cosh \lambda_k - \cos \lambda_k) \big\} \end{aligned} \tag{12}$$

where λ_k in Eq. 12 is the solution of the following equation:

$$\cos \lambda_k \cosh \lambda_k = 1 \tag{13}$$

Since $\phi_k(\xi_j)$ in Eq. 12 is orthogonal, one can normalize as:

$$\int_0^1 \phi_k^2(\xi_j) d\xi_j = 1 \tag{14}$$

Using this relationship, the arbitrary constant C_k in Eq. 12 can be defined numerically, and the matrix $\mathbf{M}_m^{ij}$ in Eq. 11 can be written as:

$$\mathbf{M}_m^{ij} = \mathbf{I}_{2k \times 2k} \tag{15}$$

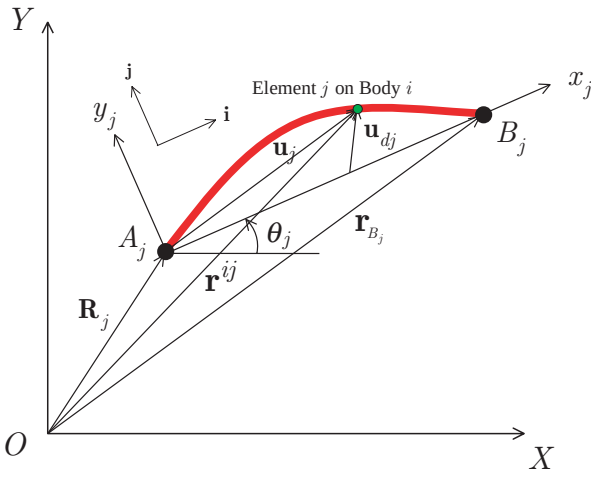

Figure 2. Deformations defined in the pinned coordinate system

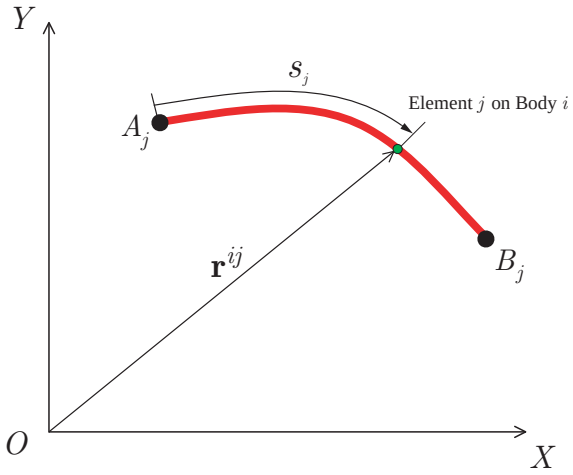

Figure 3. Deformations defined by using C.M.A

where $\mathbf{I}$ is the identity matrix. The matrices $\mathbf{M}^{ij}_{pm1}, \mathbf{M}^{ij}_{pm2}$ in Eq. 10 are coupling terms of polynomials and modes. These matrices can be analytically obtained.

Elastic Forces

There are two kinds of method to derive the element elastic forces in the previous study of A.N.C.F. One is called the pinned frame approach using the local element coordinate system that is used for the description of the element deformation as shown in Fig. 2. Another is called a continuum mechanics approach (C.M.A) that does not require the use of a local element coordinate system as shown in Fig. 3. The arc length S_j is introduced instead. The authors apply the shape function of C.M.S to these two approaches [2–5].

Pinned Frame Approach Based C.M.S In the pinned frame approach, the position vector $\mathbf{u}_j$ in Fig.2 can be written as:

$$\mathbf{u}_j = \begin{bmatrix} u_{j1} \\ u_{j2} \end{bmatrix} = \begin{bmatrix} (\mathbf{S}_1^{ij} - \mathbf{S}_{1A_j}^{ij})\,\mathbf{e}^{ij} \\ (\mathbf{S}_2^{ij} - \mathbf{S}_{2A_j}^{ij})\,\mathbf{e}^{ij} \end{bmatrix} \tag{16}$$

where $\mathbf{S}_1^{ij}$ and $\mathbf{S}_2^{ij}$ are the rows of the element shape function matrix defined in Eq. 5, and $\mathbf{S}_{1A_j}^{ij}$ and $\mathbf{S}_{2A_j}^{ij}$ are the rows of the shape function matrix defined at the reference point A_j in Fig. 2. The vector $\mathbf{u}_{dj}$ that accounts for longitudinal and transverse deflections of an arbitrary point on the beam element can be defined as:

$$\mathbf{u}_{dj} = \begin{bmatrix} u_l \\ u_t \end{bmatrix} = \begin{bmatrix} \mathbf{u}_j^T \mathbf{i} - x_j \\ \mathbf{u}_j^T \mathbf{j} \end{bmatrix} \tag{17}$$

In this study, the authors make use of the pinned frame, which has one of its axes passes through two nodes of the beam element as shown in Fig. 2. In the previous study, in comparison with the tangent frame, fewer requirements of the beam element using the pinned frame to converge well were reported in general, since the deformation within the element as defined with respect to the element coordinate system remains small despite the element large deformation [2]. The pinned frame can be introduced by first defining the unit vector $\mathbf{i}$ along a line connecting point A_j and point B_j. Therefore the unit vector $\mathbf{i}$ is:

$$\mathbf{i} = \begin{bmatrix} i_1 \\ i_2 \end{bmatrix} = \frac{\mathbf{r}_{A_j} - \mathbf{r}_{B_j}}{|\mathbf{r}_{A_j} - \mathbf{r}_{B_j}|} \tag{18}$$

Using the definition of the vector $\mathbf{e}^{ij}$ in Eq. 5, one can obtain:

$$\mathbf{i} = \frac{1}{d}\begin{bmatrix} e_5^{ij} - e_1^{ij} \\ e_6^{ij} - e_2^{ij} \end{bmatrix}, \quad d = \sqrt{(e_5^{ij} - e_1^{ij})^2 + (e_6^{ij} - e_2^{ij})^2} \tag{19}$$

where d is the distance between the nodes at A_j and B_j. Let also $\mathbf{j}$ be a unit vector along the axes of the beam coordinate system. The following relationship holds for two-dimensional problems:

$$\mathbf{j} = \tilde{\mathbf{I}}\,\mathbf{i} \tag{20}$$

where

$$\tilde{\mathbf{I}} = \begin{bmatrix} 0 & -1 \\ 1 & 0 \end{bmatrix} \tag{21}$$

Using the classical Euler-Bernoulli beam theory, the strain energy of the beam element can be written as:

$$U^{ij} = \frac{1}{2}\int_0^{l_j}\left\{EA\left(\frac{\partial u_l}{\partial x_j}\right)^2 + EI_z\left(\frac{\partial^2 u_t}{\partial x_j^2}\right)^2\right\}dx_j \tag{22}$$

where E is Young's modulus, A is the cross sectional area, I_z is the second moment of area. The variation of the strain energy can be written as:

$$\delta U^{ij} = \int_{t_1}^{t_2} \mathbf{Q}_{\mathbf{k}}^{ijT}\delta\mathbf{e}^{ij}dt \tag{23}$$

where $\mathbf{Q}_{\mathbf{k}}^{ij}$ is the vector of the element elastic forces. The elastic forces can be written more explicitly as:

$$\begin{aligned}\mathbf{Q}_{\mathbf{k}}^{ij} &= \left(\frac{\partial U^{ij}}{\partial \mathbf{e}^{ij}}\right)^T = \left(\mathbf{A}_{11}^{ij}+\mathbf{B}_{22}^{ij}\right)\mathbf{e}^{ij}i_1^2 + \left(\mathbf{A}_{22}^{ij}+\mathbf{B}_{11}^{ij}\right)\mathbf{e}^{ij}i_2^2\\ &+ \left(\mathbf{A}_{12}^{ij}+\mathbf{A}_{21}^{ij}-\mathbf{B}_{12}^{ij}-\mathbf{B}_{21}^{ij}\right)\mathbf{e}^{ij}i_2i_1 - \mathbf{A}_1^{ij}i_1 - \mathbf{A}_2^{ij}i_2\\ &+ \left\{\mathbf{e}^{ijT}\left(\mathbf{A}_{11}^{ij}+\mathbf{B}_{22}^{ij}\right)\mathbf{e}^{ij}i_1 - \mathbf{A}_1^{ijT}\mathbf{e}^{ij}\right.\\ &+ \left.\frac{1}{2}\mathbf{e}^{ijT}\left(\mathbf{A}_{12}^{ij}+\mathbf{A}_{21}^{ij}-\mathbf{B}_{12}^{ij}-\mathbf{B}_{21}^{ij}\right)\mathbf{e}^{ij}i_2\right\}\left(\frac{\partial i_1}{\partial \mathbf{e}^{ij}}\right)^T\\ &+ \left\{\mathbf{e}^{ijT}\left(\mathbf{A}_{22}^{ij}+\mathbf{B}_{11}^{ij}\right)\mathbf{e}^{ij}i_2 - \mathbf{A}_2^{ijT}\mathbf{e}^{ij}\right.\\ &+ \left.\frac{1}{2}\mathbf{e}^{ijT}\left(\mathbf{A}_{12}^{ij}+\mathbf{A}_{21}^{ij}-\mathbf{B}_{12}^{ij}-\mathbf{B}_{21}^{ij}\right)\mathbf{e}^{ij}i_1\right\}\left(\frac{\partial i_2}{\partial \mathbf{e}^{ij}}\right)^T\end{aligned} \tag{24}$$

Each coefficient of matrices in Eq. 24 ($r, s = 1, 2$) can be written as:

$$\mathbf{A}_{rs}^{ij} = \frac{EA}{l_j}\int_0^1\left(\frac{\partial \mathbf{S}_r^{ij}}{\partial\xi_j}\right)^T\left(\frac{\partial \mathbf{S}_s^{ij}}{\partial\xi_j}\right)d\xi_j \tag{25}$$

$$\mathbf{B}_{rs}^{ij} = \frac{EI_z}{l_j^3}\int_0^1\left(\frac{\partial^2 \mathbf{S}_r^{ij}}{\partial\xi_j^2}\right)^T\left(\frac{\partial^2 \mathbf{S}_s^{ij}}{\partial\xi_j^2}\right)d\xi_j \tag{26}$$

$$\mathbf{A}_r^{ij} = EA\int_0^1\left(\frac{\partial \mathbf{S}_r^{ij}}{\partial\xi_j}\right)^T d\xi_j \tag{27}$$

The authors list typical matrices in Eqs. 25 - 27 as follows:

$$\int_0^1\left(\frac{\partial \mathbf{S}_{p1}^{ij}}{\partial\xi_j}\right)^T\left(\frac{\partial \mathbf{S}_{p1}^{ij}}{\partial\xi_j}\right)d\xi_j \equiv \mathbf{K}_A^{ij} \tag{28}$$

$$\int_0^1\left(\frac{\partial^2 \mathbf{S}_{p1}^{ij}}{\partial\xi_j^2}\right)^T\left(\frac{\partial^2 \mathbf{S}_{p1}^{ij}}{\partial\xi_j^2}\right)d\xi_j \equiv \mathbf{K}_B^{ij} \tag{29}$$

$$\int_0^1\left(\frac{\partial \mathbf{S}_{p1}^{ij}}{\partial\xi_j}\right)^T\left(\frac{\partial \mathbf{\Phi}_{m1}^{ij}}{\partial\xi_j}\right)d\xi_j \equiv \mathbf{K}_C^{ij} \tag{30}$$

$$\int_0^1\left(\frac{\partial \mathbf{\Phi}_{m1}^{ij}}{\partial\xi_j}\right)^T\left(\frac{\partial \mathbf{\Phi}_{m1}^{ij}}{\partial\xi_j}\right)d\xi_j \equiv \mathbf{K}_D^{ij} \tag{31}$$

$$\int_0^1\left(\frac{\partial^2 \mathbf{S}_{p1}^{ij}}{\partial\xi_j^2}\right)^T\left(\frac{\partial^2 \mathbf{\Phi}_{m1}^{ij}}{\partial\xi_j^2}\right)d\xi_j \equiv \mathbf{K}_E^{ij} \tag{32}$$

$$\int_0^1\left(\frac{\partial^2 \mathbf{\Phi}_{m1}^{ij}}{\partial\xi_j^2}\right)^T\left(\frac{\partial^2 \mathbf{\Phi}_{m1}^{ij}}{\partial\xi_j^2}\right)d\xi_j \equiv \mathbf{K}_F^{ij} \tag{33}$$

Shabana [1] derived matrices $\mathbf{K}_A^{ij}$ and $\mathbf{K}_B^{ij}$ in Eqs. 28 and 29 by integrating the products of shape function $\mathbf{S}_p^{ij}$ as:

$$\mathbf{K}_A^{ij} = \begin{bmatrix} \frac{6}{5} & \frac{l_j}{10} & -\frac{6}{5} & \frac{l_j}{10} \\ & \frac{2l_j^2}{15} & -\frac{l_j}{10} & -\frac{l_j^2}{30} \\ & & \frac{6}{5} & -\frac{l_j}{10} \\ Sym & & & \frac{2l_j^2}{15} \end{bmatrix} \tag{34}$$

$$\mathbf{K}_B^{ij} = \begin{bmatrix} 12 & 6l_j & -12 & 6l_j \\ & 4l_j^2 & -6l_j & 2l_j^2 \\ & & 12 & -6l_j \\ Sym & & & 4l_j^2 \end{bmatrix} \tag{35}$$

The matrices $\mathbf{K}_C^{ij}$, $\mathbf{K}_D^{ij}$, $\mathbf{K}_E^{ij}$ and $\mathbf{K}_F^{ij}$ in Eqs. 30 – 33 are also derived in the same manner and can be analytically obtained.

Continuum Mechanics Approach Based C.M.S In the preceding section, the formulation of the elastic forces based on C.M.S using a local element coordinate system was discussed. However, in A.N.C.F, it is not necessary to use such a local coordinate system. As discussed in the previous study based on C.M.A [5, 6], Eq. 1 is the parametric equation of a two-dimensional line. Thus the configuration of a beam element at time t as shown in Fig. 3 can be defined as:

$$\mathbf{r}^{ij} = \mathbf{r}^{ij}(x_j), \qquad 0 \le x_j \le l_j \tag{36}$$

The arc length S_j in Fig. 3 is related to x_j through the differential equation as:

$$dS_j = \sqrt{\mathbf{r}^{ij\prime T}\mathbf{r}^{ij\prime}}dx_j, \quad \mathbf{r}^{ij\prime} = \frac{d\mathbf{r}^{ij}}{dx_j} \tag{37}$$

The Green-Lagrange longitudinal strain ε_l^{ij} can be defined using the following equation:

$$dS_j^2 - dx_j^2 = 2dx_j \varepsilon_l^{ij} dx_j \tag{38}$$

which implies that

$$\varepsilon_l^{ij} = \frac{1}{2}(\mathbf{r}^{ij\prime T}\mathbf{r}^{ij\prime} - 1) \tag{39}$$

This equation can be written in terms of the vector of nodal coordinates $\mathbf{e}^{ij}$ using Eqs. 2 and 3 as:

$$\varepsilon_l^{ij} = \frac{1}{2}(\mathbf{e}^{ijT}\mathbf{S}^{ij\prime T}\mathbf{S}^{ij\prime}\mathbf{e}^{ij} - 1) \tag{40}$$

The longitudinal deformation may be related to longitudinal stresses by specifying the constitutive equations. Using the classical Euler-Bernoulli beam theory, the vector of generalized elastic forces due to the longitudinal deformation can be defined as:

$$\mathbf{Q}_l^{ij} = \left(\frac{\partial U_l^{ij}}{\partial \mathbf{e}^{ij}}\right)^T = \int_0^{l_j} EA\varepsilon_l^{ij}\mathbf{S}^{ij\prime T}\mathbf{S}^{ij\prime}\mathbf{e}^{ij}dx_j \tag{41}$$

From this equation, it is clear that if the length of the finite element is small enough to consider ε_l^{ij} as constant, then it is possible to factor it out of the sign of integral as follows:

$$\mathbf{Q}_l^{ij} = EA\bar{\varepsilon}_l^{ij}\left[\int_0^{l_j} \mathbf{S}^{ij\prime T}\mathbf{S}^{ij\prime}dx_j\right]\mathbf{e}^{ij} \tag{42}$$

where $\bar{\varepsilon}_l^{ij}$ is the average longitudinal strain which can be approximated as:

$$\bar{\varepsilon}_l^{ij} = \frac{d - l_j}{l_j} \tag{43}$$

In Eq. 43, d is defined as Eq. 19. The elastic force vector $\mathbf{Q}_l^{ij}$ due to the longitudinal deformation can be written as:

$$\mathbf{Q}_l^{ij} = \mathbf{K}_l^{ij}\mathbf{e}^{ij} \tag{44}$$

where

$$\mathbf{K}_l^{ij} = \frac{EA}{l_j}\bar{\varepsilon}_l^{ij}\begin{bmatrix} \mathbf{K}_A^{ij} & \mathbf{0} & \mathbf{K}_C^{ij} & \mathbf{0} \\ \mathbf{0} & \mathbf{K}_A^{ij} & \mathbf{0} & \mathbf{K}_C^{ij} \\ \mathbf{K}_C^{ijT} & \mathbf{0} & \mathbf{K}_D^{ij} & \mathbf{0} \\ \mathbf{0} & \mathbf{K}_C^{ijT} & \mathbf{0} & \mathbf{K}_D^{ij} \end{bmatrix} \tag{45}$$

The effect of bending moments can be introduced using the curvature κ of the beam element as:

$$M = EI_z\kappa \tag{46}$$

The Serret-Frenet formulas of differential geometry give:

$$\kappa = \left|\frac{d^2\mathbf{r}^{ij}}{dS_j^2}\right| \approx \left|\frac{d^2\mathbf{r}^{ij}}{dx_j^2}\right| = \left|\mathbf{r}^{ij\prime\prime}\right| \tag{47}$$

In this equation, the special assumption of small longitudinal deformations ($S_j \approx x_j$) is employed. The strain energy U_t^{ij} accounting for bending deformations is given by:

$$U_t = \frac{1}{2}\int_0^{l_j} EI_z\kappa^2 dx_j = \frac{1}{2}\mathbf{e}^{ijT}\mathbf{K}_t^{ij}\mathbf{e}^{ij} \tag{48}$$

The elastic force vector $\mathbf{Q}_t^{ij}$ due to the transverse deformation can be written as:

$$\mathbf{Q}_t^{ij} = \mathbf{K}_t^{ij}\mathbf{e}^{ij} \tag{49}$$

where

$$\mathbf{K}_t^{ij} = \frac{EI_z}{l_j^3}\begin{bmatrix} \mathbf{K}_B^{ij} & \mathbf{0} & \mathbf{K}_E^{ij} & \mathbf{0} \\ \mathbf{0} & \mathbf{K}_B^{ij} & \mathbf{0} & \mathbf{K}_E^{ij} \\ \mathbf{K}_E^{ijT} & \mathbf{0} & \mathbf{K}_F^{ij} & \mathbf{0} \\ \mathbf{0} & \mathbf{K}_E^{ijT} & \mathbf{0} & \mathbf{K}_F^{ij} \end{bmatrix} \tag{50}$$

Using Eqs. 44 and 49, the final expression of the elastic forces in Eq. 23 is given by:

$$\mathbf{Q}_{\mathbf{k}}^{ij} = \mathbf{Q}_l^{ij} + \mathbf{Q}_t^{ij} \tag{51}$$

The elastic forces in C.M.S based beam element are obtained by the same manner to the conventional C.M.A [2, 6] but includes the analytical mode shape functions.

Element Equations of Motion and Constrained Multibody Equations

The equations of motion of element j on body i can be written as follows [12, 13]:

$$\mathbf{M}^{ij}\ddot{\mathbf{e}}^{ij} = \mathbf{F}_e^{ij} + \mathbf{F}_c^{ij} \tag{52}$$

where $\mathbf{F}_e^{ij} = \mathbf{Q}_\mathbf{a}^{ij} - \mathbf{Q}_\mathbf{k}^{ij}$ is a vector which includes all the element external and applied force vector $\mathbf{Q}_\mathbf{a}^{ij}$ including the gravity forces and the element elastic forces $\mathbf{Q}_\mathbf{k}^{ij}$ due to deformations. $\mathbf{F}_c^{ij}$ is the vector of constraint forces resulting from connectivity between the finite beam elements. Using a conventional finite element assembly procedure also based on C.M.S, the equations of motion for body i can be written as:

$$\mathbf{M}^i \ddot{\mathbf{e}}^i = \mathbf{F}_e^i \tag{53}$$

where $\mathbf{e}^i$ is the vector of nodal coordinates of body i. $\mathbf{M}^i$ and $\mathbf{F}_e^i$ are the assembled mass matrix and the external and elastic force vector of the body, respectively. In Eq. 53, the constraint forces due to the element connectivity are eliminated. If the body i is subjected to kinematic constraints resulting from mechanical joints, specified motion trajectories, the equations of motion of the body i can be written as:

$$\mathbf{M}^i \ddot{\mathbf{e}}^i + \mathbf{C}_{\mathbf{e}^i}^T \boldsymbol{\lambda} = \mathbf{F}_e^i, \qquad i = 1, 2, \ldots, n_b \tag{54}$$

where $\boldsymbol{\lambda}$ is the vector of Lagrange multipliers, $\mathbf{C}$ is the vector of constraint functions that depend on the coordinates and possibly on time, $\mathbf{C}_{\mathbf{e}^i}$ is the constraint Jacobian matrix associated with the vector of nodal coordinates of the deformable body i and n_b is the total number of bodies. Since the mass matrix $\mathbf{M}^i$ of the C.M.S based beam element in this study is constant and symmetric, a Cholesky velocity transformation [12, 13] can be used to obtain a generalized identity mass matrix. Finally the resulting augmented form of the equations of motion can be written as:

$$\begin{bmatrix} \mathbf{I} & \mathbf{C}_{\mathbf{q}_{ch}}^T \\ \mathbf{C}_{\mathbf{q}_{ch}} & \mathbf{0} \end{bmatrix} \begin{bmatrix} \ddot{\mathbf{q}}_{ch} \\ \boldsymbol{\lambda} \end{bmatrix} = \begin{bmatrix} \mathbf{Q}_{ch} \\ \mathbf{Q}_c \end{bmatrix} \tag{55}$$

where $\mathbf{C}_{\mathbf{q}_{ch}}$ is the constraint Jacobian matrix associated with the vector of the Cholesky coordinates $\mathbf{q}_{ch}$, $\mathbf{Q}_{ch}$ is the generalized Cholesky forces and $\mathbf{Q}_c$ is a quadratic velocity vector.

NUMERICAL EXAMPLES

In this section, four numerical examples including spin-up maneuver, flexible cantilever beam, slider crank mechanism and four bar mechanism are investigated in order to demonstrate the use of the proposed method based on C.M.S in case of not only the small deformation but also the large rotation and large deformation problem. The authors provide five models, Model A, B, C, D and E. Model A, B and C are based on C.M.S, and Model D and E are based on the conventional A.N.C.F. In all examples, denoted as Model A based on a pinned frame approach is extended to C.M.S model. Model B and C are based on C.M.A (which corresponds to Model I of [6] and the model of [5]) extended to C.M.S model, respectively. Both Model D and Model E are comparative models not extended to C.M.S model. Model D is based on C.M.A (which corresponds to Model III of [6]). Model E is based on a pinned frame approach [2–4].

Spin-Up Maneuver In this example, the spin-up maneuver of a rotating beam is employed to investigate how accurate the beam element proposed in this study is with the totally reduced system degrees of freedom in case of small deformation undergoes large rotation. To compare with the previous formulation [14, 15] of a rotating beam of length $L = 8.0$ m, density $\rho = 2.767 \times 10^3$ kg/m^3, cross sectional area $A = 7.299 \times 10^{-5}$ m^2, and bending stiffness $EI_z = 5.664 \times 10^2$ Nm^2 in the example of [14], and $L = 10$, $\rho A = 1.2$, $EA = 2.8 \times 10^7$ and $EI_z = 1.4 \times 10^4$ in the example of [15], the shaft is given an angular displacement $\theta(t)$ about the global Z axis, defined as:

$$\theta(t) = \begin{cases} \dfrac{\omega_s}{T_s}\left[\dfrac{1}{2}t^2 + \left(\dfrac{T_s}{2\pi}\right)^2 \left(\cos\left(\dfrac{2\pi t}{T_s}\right) - 1\right)\right], & t < T_s \\ \omega_s\left(t - \dfrac{T_s}{2}\right), & t \geq T_s \end{cases} \tag{56}$$

where ω_s and T_s are set to 4.0 rad/sec and 15 sec, respectively in the example of [14], and to 6.0 rad/sec and 15 sec in the example of [15]. Figures 4 and 5 show the transverse and longitudinal deflections of the rotating beam at the free end.

The results presented in these figures show that there is a good agreement between the present models and the conventional models. In Fig. 4, Model B has one beam element with one C.M.S vibration mode, while Model D has two beam elements. In case of Fig. 5, Model B has two beam elements with two vibration modes, while Model D has five beam elements. The results obtained in this example show that presented method based on C.M.S gives a good agreement with the results obtained by only using A.N.C.F. In addition to this fact, a steady state extension at the free end of 5.14×10^{-4} can be also confirmed as shown in Fig. 5. Model D is chosen to be a comparative model in this example because of its high accuracy in the case of large longitudinal deformation [6]. The total CPU time used to obtain the solution on a Mobile AMD Athlon 4 Processor 1.10 GHz using MATLAB is 133 sec (Model B) and 1656 sec (Model D) in the example of [14] and 907 sec (Model B) and 9604 sec (Model D) in the example of [15], respectively.

Flexible Cantilever Beam In this example, the accuracy with reduced system degrees of freedom is examined by using small numbers of finite elements in case of large deformation. The authors consider a flexible cantilever beam [4] assumed

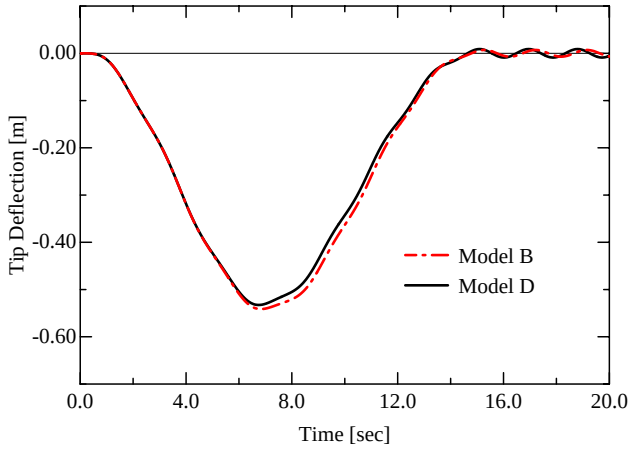

Figure 4. Transverse deflection at the free end of the rotating beam in case of Wu and Haug, 1988

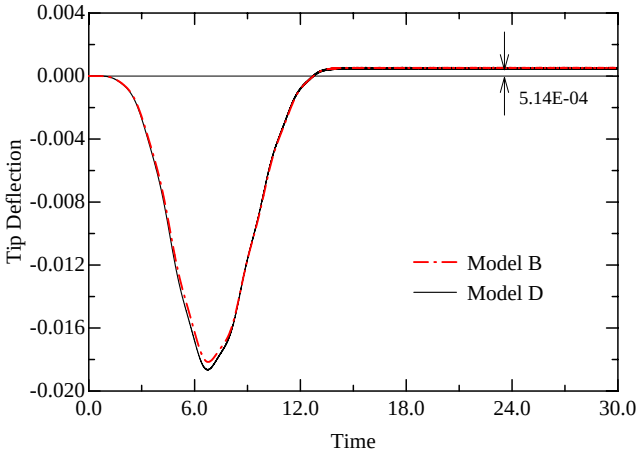

Figure 5. Longitudinal deflection at the free end of the rotating beam in case of Simo and Vu-Quoc, 1986

to be subjected to a vertical concentrated force $F_0 = 0.09$ N in the following equation.

$$F(t) = \begin{cases} \dfrac{F_0}{2}\,(1-\cos(\pi t)), & t < 1\text{sec} \\ F_0, & t \geq 1\text{sec} \end{cases} \qquad (57)$$

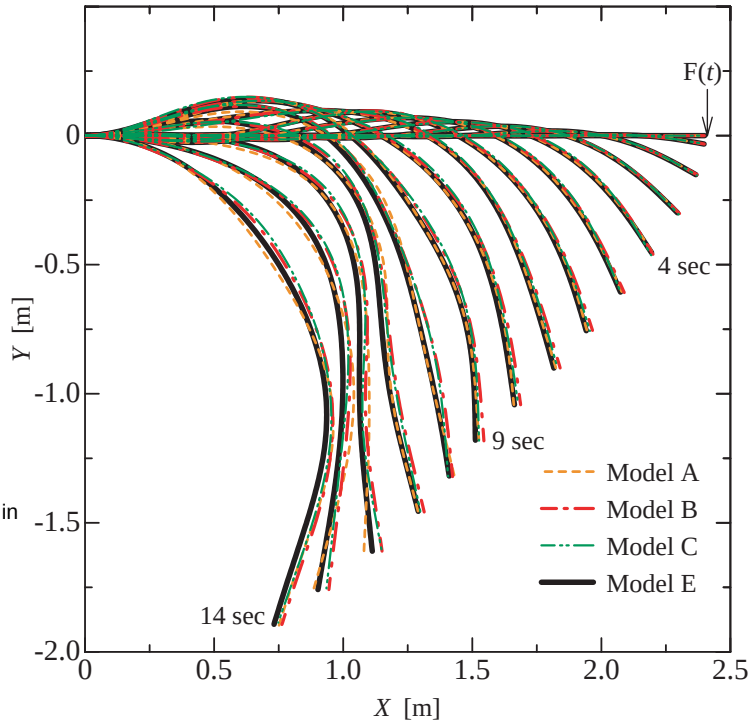

Figure 6. Deformation of a flexible cantilever beam subject to a concentrated force at the same time step of 1.0 sec

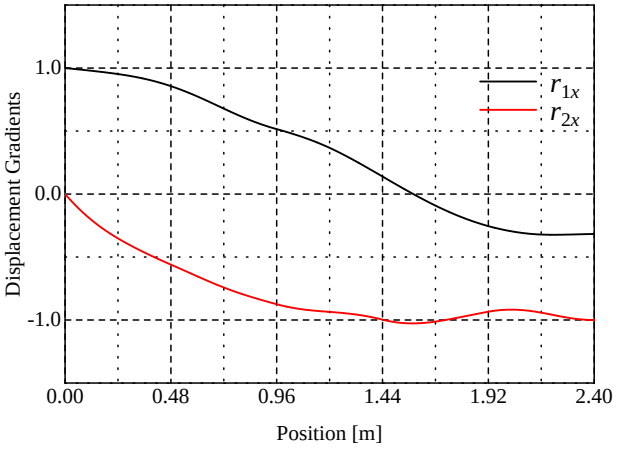

Figure 7. Components of the vector $\dfrac{\partial \mathbf{r}}{\partial x}$ at time 14 sec

The beam has a length of 2.4 m, a cross sectional area of 0.0018 m^2, a second moment of area 1.215×10^{-8} m^4, a mass density of 2770 kg/m^3 and a modulus of elasticity of 1.000×10^6 N/m^2, respectively. Figure 6 shows the configurations of the beam at the same time step of 1.0 sec. In this figure, Model A has ten beam elements with one vibration mode, Model B has five beam elements with two vibration modes, Model C has five beam elements with one vibration mode and Model E has thirty beam elements, respectively. In this case, good agreements in deformation are found between the results obtained by three C.M.S based beam elements, Model A, B and C, and the element obtained by the conventional A.N.C.F, Model E. Model C has 34 dof while

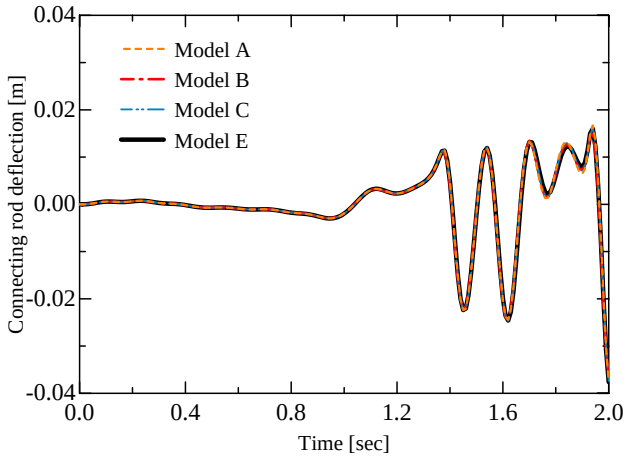

Figure 8. Deformation of the midpoint of the connecting rod in case of Slider Crank Mechanism

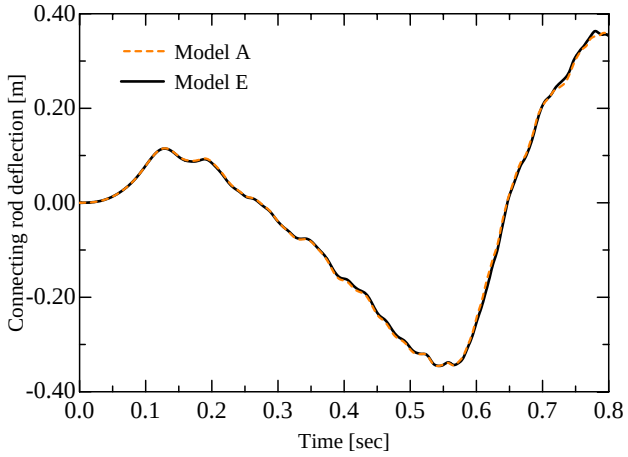

Figure 9. Deformation of the midpoint of the connecting rod in case of Four Bar Mechanism

Model E has 124 dof. Then, the high precision reduced order formulation by C.M.S is realized in the sense that the solutions obtained by using C.M.S are comparatively similar to the conventional ones obtained by only using A.N.C.F.

Figure 7 shows the components of the vector $\partial \mathbf{r}/\partial x$ along the center line of the beam element at time 14 sec of Model B. This result demonstrates that the global displacement gradients at each nodal point are continuous since the beam element proposed in this study is modeled by using the conformal global shape function and the analytical clamped-clamped beam modes that satisfy not only zero displacement but also zero slope at each node, respectively. In Fig. 7, the deformation of the center line can be measured by the deviation of the norm of the vector $\partial \mathbf{r}/\partial x$ from one, since this vector is not an orthogonal unit vector in

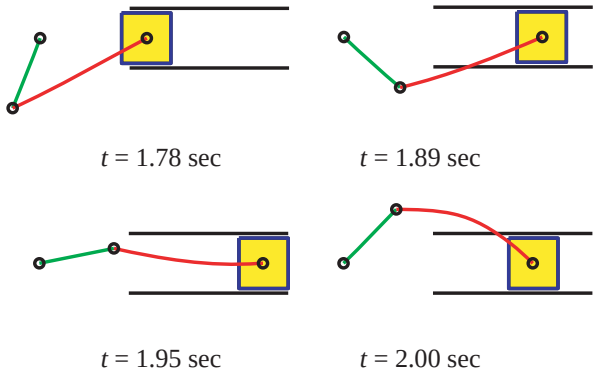

Figure 10. Computer Animation of Slider Crank Mechanism (Model B)

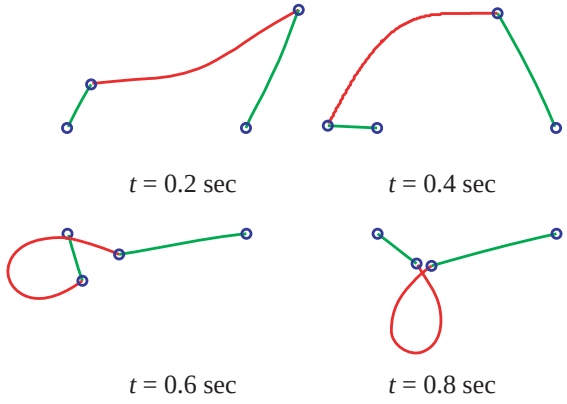

Figure 11. Computer Animation of Four Bar Mechanism (Model A)

case of large deformation. The total CPU time used to obtain the solution is 1460 sec (Model A), 126 sec (Model B), 85 sec (Model C) and 61452 sec (Model E), respectively.

Flexible Slider Crank & Four Bar Mechanism In this example, we consider two simulations using C.M.S based beam element. One is the very flexible slider crank mechanism investigated in [3], the other is the very flexible four bar mechanism investigated in [2]. In each case, the beam element has the same length, cross sectional dimensions and material properties as a crank shaft, a connecting rod and a follower (in case of four bar mechanism) in comparison with the case of [2, 3]. Figures 8 and 9 show the connecting rod deflections of midpoints. In case of slider crank simulation, Model A has four beam elements with one vibration mode (total 36 dof), Model B has two beam elements with three vibration modes (total 32 dof), Model C has four beam elements with one vibration mode (total 36 dof), and Model E has eight beam elements as a connecting rod (total 52 dof). In this case, Model A and C have the same numbers of degrees of freedom. In Model A, B and C, the crank shaft

has one beam element, while in Model E, it has three beam elements. In case of four bar mechanism, all models have one beam element and four beam elements as a crankshaft and a follower. Model A has ten beam elements with two vibration modes (total 112 dof), while Model E has twenty four beam elements (total 128 dof) as a connecting rod. There is a very good agreement between each model as shown in Figs. 8 and 9. Figures 10 and 11 show the computer animation of slider crank (Model B) and four bar mechanism (Model A). As a consequence, we can reduce the number of system degrees of freedom by maximum 20 dof in case of slider crank mechanism and 16 dof in case of four bar mechanism. The total CPU time used to obtain the solution is 1794 sec (Model A), 204 sec (Model B), 310 sec (Model C) and 9264 sec (Model E) in Fig. 8 and 5853 sec (Model A) and 20695 sec (Model E) in Fig. 9, respectively.

SUMMARY AND CONCLUSIONS

In this study, the beam element based on A.N.C.F is developed to realize higher efficiency and higher accuracy model with the less number of elements and system coordinates. The deformation is modeled by using the global shape function and the analytical clamped-clamped beam modes that ensure the continuity of all the displacements and displacement gradients at nodal points and the smoothness of the center line. The shape function proposed in this study satisfies both the compatibility conditions and the completeness conditions which imply one of the sufficient conditions for the convergence of finite element. The present beam element belongs to the type of C^1 element which requires slope continuity. Four numerical examples are investigated in order to examine the validity of the present C.M.S beam model. We can confirm a very good agreement between the low order C.M.S model and the large number of element types.

ACKNOWLEDGMENT

The authors wish to thank Professor. A.A. Shabana of University of Illinois at Chicago for his kind advice about the numerical techniques.

REFERENCES

[1] Shabana, A. A., 1998a, *Dynamics of Multibody Systems*, 2^{nd} ed., Cambridge University Press.

[2] Berzeri, M., Campanelli, M., and Shabana, A. A., 2001, "Definition of the Elastic Forces in the Finite-Element Absolute Nodal Coordinate Formulation and the Floating Frame of Reference Formulation," Multibody System Dynamics, **5**, pp. 21–54.

[3] Escalona, J. L., Hussien, H. A., and Shabana, A. A., 1998, "Application of the Absolute Nodal Coordinate Formulation to Multibody System Dynamics," Journal of Sound and Vibration, **214**, No. 5, pp. 833–851.

[4] Shabana, A. A., Hussien, H. A., and Escalona, J. L., 1998, "Application of the Absolute Nodal Coordinate Formulation to Large Rotation and Large Deformation Problems," ASME Journal of Mechanical Design, **120**, pp. 188–195.

[5] Takahashi, Y., and Shimizu, N., 1999, "Study on Elastic Forces of the Absolute Nodal Coordinate Formulation for Deformable Beams," presented at the *Second Symposium on Multibody Dynamics and Vibration, ASME Conferences*, Las Vegas, Paper # DETC99/VIB-8203.

[6] Berzeri, M., and Shabana, A. A., 2000, "Development of Simple Models for the Elastic Forces in the Absolute Nodal Coordinate Formulation," Journal of Sound and Vibration, **235** (4), pp. 539–565.

[7] Omar, M. A., and Shabana, A. A., 2000, "Development of a Shear Deformable Element Using the Absolute Nodal Coordinate Formulation," Technical Report MBS00-3-UIC, University of Illinois at Chicago, Chicago,IL.

[8] Mikkola, A. M., and Shabana, A. A., 2000, "A Large Deformation Plate Element for Multibody Applications," Technical Report MBS00-6-UIC, University of Illinois at Chicago, Chicago,IL.

[9] Shabana, A. A., and Yakoub, R. Y., 2000, "An Isoparametric Three Dimensional Beam Element Using The Absolute Nodal Coordinate Formulation" Technical Report MBS00-1-UIC, University of Illinois at Chicago, Chicago,IL.

[10] Kobayashi, N., 1989, "Modeling Methodology of Beam Structure for Vibration Suppression Control (in Japanese)," Proceedings of JSME, 890-61, pp. 86–87.

[11] Kobayashi, N., Sugiyama, H., and Watanabe, M., 2001, "Dynamics of Flexible Beam using a Component Mode Synthesis based Formulation," Proceedings of the ASME 2001 Design Engineering Technical Conferences, Pittsburgh, PA, September 2001, Paper # DETC2001/VIB-21351.

[12] Shabana, A. A., 1998b, "Computer Implementation of the Absolute Nodal Coordinate Formulation for Flexible Multibody Dynamics," Journal of Nonlinear Dynamics, **16**, pp. 293–306.

[13] Yakoub, R. Y., and Shabana, A. A., 1999, "Use of Cholesky Coordinates and the Absolute Nodal Coordinate Formulation in the Computer Simulation of Flexible Multibody Systems," Journal of Nonlinear Dynamics, **20**, pp. 267–282.

[14] Wu, S. C., and Haug, E. J., 1988, "Geometric Nonlinear Substructuring for Dynamics and Flexible Mechanical Systems," International Journal of Numerical Methods in Engineering, **26**, pp. 2211–2226.

[15] Simo, J. C., and Vu-Quoc, L., 1986, "On the Dynamics of Flexible Beams Under Large Overall Motion-the Plane Case: Part I and II," ASME Journal of Applied Mechanics, **53**, pp. 849–863.